

## Calibrations

Various calibration procedures are performed for trend analysis purposes; they are mainly used by the instrument scientist. They include a control of the slit position with respect to the detector, calibration of the spectroscopic dispersion relation with calibration lamps, analysis of known spectral lines to correct for spectrum tilts or curvature in the spatial direction, and spectroscopic flat-fields.

## Observations

Spectroscopic observations performed with the *NodOnSlit* template produce spectra on two different positions A and B obtained by a shift of the telescope along the slit. Each set of images is averaged to a single image, and both sets are subtracted from each other. Available outputs are images of (A-B), (B-A), and a combined image of those two. The com-

bined image is actually the most important one for the observer, since extraction will take place on this 2d-spectrum image. The pipeline goes on from this point, extracting the brightest spectrum from this image, performs flux and wavelength calibrations when adequate calibration data are available, and outputs the results to a FITS table.

The brightest spectrum is to be seen as a checkpoint: since it is usually a reference object, it might be useful to check out that the acquisition actually performed as expected at least on this object. This spectrum is available to the user in the control room, together with the combined 2d image so that spectrum extraction can proceed from that point (partly) by hand.

Notice that spectroscopy recipes should be distributed as a part of MIDAS in a subset dedicated to pipeline routines. Some are supporting an interactive mode that actually allows giving more indica-

tions about how the procedure runs and lead them to proceed directly to the solution for the spectra of interest.

## Acknowledgements

All ISAAC pipeline data reduction algorithms are based on the ISAAC calibration plan (ESO document VLT-PLA-ESO-14100-1384) by Pierre-Alain Duc and Jean-Gabriel Cuby. All procedures have been improved tremendously following the advice from Chris Lidman. Numerous discussions with Alan Moorwood, Almudena Prieto, Paola Amico, Pascal Ballester have helped a lot to clarify the requirements and improve the spectroscopy parts. The jitter process has received constructive and helpful comments from too many people to quote them all here; we thank them for their contributions.

ndevil@eso.org

# Commissioning FEROS, the New High-resolution Spectrograph at La Silla

A. KAUFER, O. STAHL, S. TUBBESING, Landessternwarte Heidelberg-Königstuhl  
P. NØRREGAARD, Astronomical Observatory Copenhagen  
G. AVILA, P. FRANCOIS, L. PASQUINI, A. PIZZELLA, ESO

## Introduction

On November 30, 1998, the second commissioning phase of the new Fiberfed Extended Range Optical Spectrograph (FEROS) was completed at the ESO 1.52-m telescope at La Silla.

The instrument had been installed by a small team from the Heidelberg, Copenhagen and La Silla observatories starting in mid-September – just two years after the contract signature between the FEROS consortium and ESO. FEROS saw its first stellar light at the end of the installation phase on October 6th.

An overview of the design and of the expected capabilities of the FEROS instrument has been presented in a previous paper [Kaufer et al., 1997, *The Messenger* 89, 1]; a more detailed description of the opto-mechanical design is found in [Kaufer & Pasquini, 1998, Proc. SPIE Vol. 3355, p. 844]. In the present article, the major technical results from the two commissioning phases which followed the first light event are reported.

## The Spectrograph Environment

Figure 1 shows the FEROS spectrograph inside its temperature and humidity controlled room, which was erected by the La Silla infrastructure team at the place of the former Echelec spectrograph inside the coudé room of the ESO 1.52-m telescope. The feet of the optical

bench are sitting on a platform coupled to the telescope pier but decoupled from the room's floor. The LN<sub>2</sub> supply tank is located outside of the spectrograph room in the neighbouring FEROS maintenance room and can be replaced every two weeks without entering the spectrograph room. Adding to these facts the very stable temperature which is maintained inside the room ( $\Delta T < 0.2$  K over 1 night), FEROS is located in a very stable environment – a crucial prerequisite for a long-term stability of the instrument as required for high-precision spectroscopic measurements.

From the spectrograph, the two fibers together with their metallic protection cable are led through the telescope's polar and declination axes, further inside the telescope's double tube, and eventually leave the telescope and enter the Boller & Chivens (B&C) Cassegrain spectro-

graph to end in the telescope's focal plane, which now hosts the new FEROS fiber head and the previous B&C long slit.

## Instrument Performance

Table 1 summarises some of the main performances of FEROS as determined during the commissioning.

## Efficiency

The detection efficiency of the complete system ESO 1.52-m telescope + fiber link + FEROS + Detector has been measured several times under photometric conditions using bright and faint CTIO standard stars [Hamuy et al., 1994, *PASP*, 106, 566]. Correction for the atmospheric extinction has been made according to the standard La Silla extinction tables. The typically achieved detection

Table 1: Measured performance of FEROS.

Wavelength Range in one exposure (object+sky)	360 – 920 nm (39 orders, 2 fibers)
Resolving Power	$\lambda/\Delta\lambda = 48,000$ (2.2 pixels)
Entrance Aperture	2.7 arcsec (circular)
Detection Efficiency (with telescope and detector)	1% at 360 nm, 16% at 440 nm, 17% at 550 nm 16% at 640 nm, 11% at 790 nm
Limiting Magnitudes at the ESO 1.52	16 mag in V, S/N = 9, $t_{\text{exp}} = 2$ h 12 mag in V, S/N = 105, $t_{\text{exp}} = 2$ h
Radial-Velocity Accuracy	21 m/s rms (2-month time base)
Inter-order straylight	< 3%

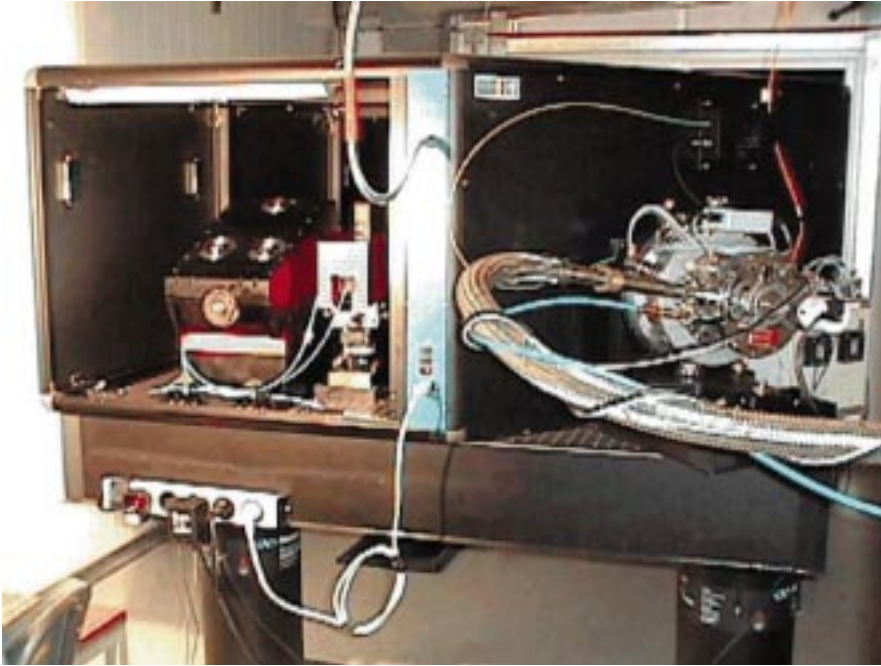


Figure 1: FEROS in the FEROS room at La Silla. One cover has been removed, which allows to see the echelle mount on the left with the fiber exit unit next to it. On the right is the detector system with the LN<sub>2</sub> supply line of the continuous-flow cryostat in the front.

efficiencies in the *UBVRI* colours are given in Table 1. The peak system efficiency of 17% considerably exceeds the performance of most (if not all) of the currently operating high-resolution spectrographs.

The high throughput together with the large simultaneous wavelength coverage from 360 to 920 nm in 39 orders for both fibers and the high resolving power of  $R = 48,000$  reflect the outstanding performance of this new ESO instrument.

The measured spectrograph efficiency is consistent with the computations from the design and construction phase as can be seen in Figure 2. The efficiency in the very blue below 400 nm is lower than expected in the Final Design Report. This is due to the reflective coating of the mirrors which performs in this spectral range only at the lower limit of its specification. Since the optical path goes through four reflections on this coating, a drop of the efficiency in the blue becomes noticeable.

### Spectral Resolution

The measured spectral resolving power of FEROS is  $R = 48,000$  corresponding to 2.2 pixels of 15  $\mu\text{m}$ . This resolution is achieved with the help of the two-beam two-slice image slicer [Kaufner, 1998, Fiber Optics in Astronomy III, ASP Conf. Series 152, 337]. The width and asymmetry of about 500 selected calibration lamp emission lines over the full echelle frame are routinely measured by the data reduction software. The FWHMs of the lines show a maximum degradation of < 15% in the extreme corners of the CCD. Along the dispersion direction a slight trend of the line widths is visible which presumably is due to a residual tilt of the CCD detector with respect to the

field lens. The necessary alignment is planned to be carried out during an outstanding CCD upgrade (see below). The asymmetries of the lines are described by Gauss-Hermite polynomials and are below 1% for the odd and even terms.

### Straylight and Ghosts

The inter-order straylight is primarily produced by the echelle grating and the

roughness of the optical surfaces. The straylight distribution is found to be very local, i.e., it follows the intensity distribution of the spectral light source in the orders. This result was not clear *a priori* for the white pupil design used in FEROS. With this, we could determine the straylight level with the help of flatfield exposures by comparing the intensities in the orders with the intensities of the inter-order background: the straylight levels are found to be less than 3% all over the CCD.

The straylight contamination along the orders is difficult to determine. Therefore, we compared several very deep absorption lines of FEROS solar spectra with Kitt-Peak FTS spectra. After matching the resolution and pixelisation of the spectra, no considerable (> 2%) filling of the cores of the spectral lines was observed.

Several tests were carried out to identify possible ghost images produced in the optical system of FEROS. A spectrum of the emission line star  $\eta$  Carinae with a highly saturated H $\alpha$  line revealed the presence of a focalised ghost image of this H $\alpha$  line between two orders close to the centre of the CCD. The relative intensity level of this ghost was measured to  $5 \times 10^{-4}$  which is not critical.

### Fiber Flatfield Stability

During the construction of FEROS, different teams reported on problems with the stability of flatfields in fiber-fed high-resolution spectrographs [e.g. Baudrand et al., 1998, ASP Conf. Series 152, 32] limiting the maximum achievable S/N in stellar spectra down to about 200. Since it was not possible to pin down the reason for this degradation, FEROS had to

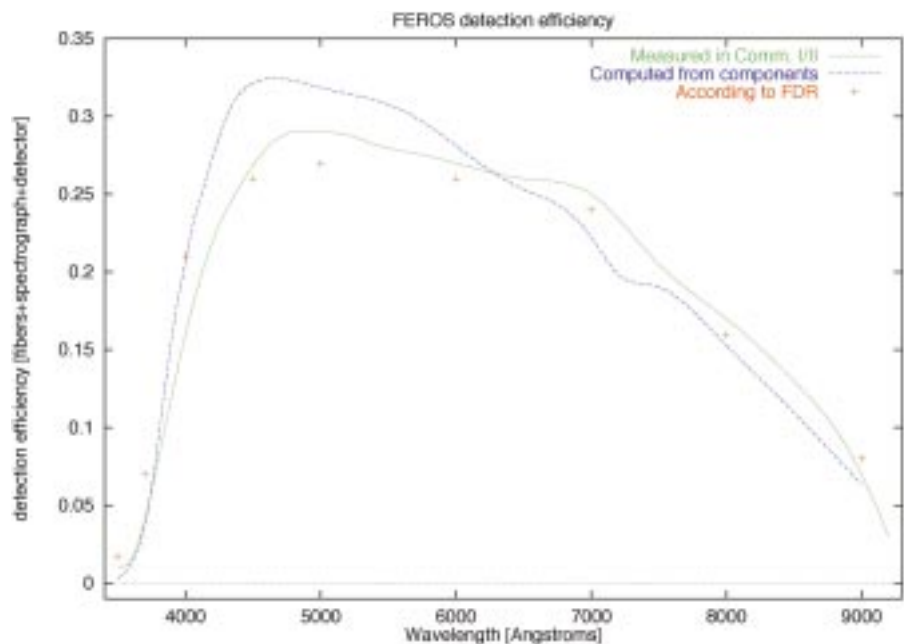


Figure 2: Efficiency of FEROS fibers + spectrograph + detector. The efficiency curve is derived from a spectrum of the standard star HR 9087. For the atmospheric extinction correction the standard La Silla extinction tables were used; for the telescope, an efficiency of 60% is assumed. The red crosses give the expected efficiency according to the FEROS Final Design Report (FDR); the blue curve is the total efficiency computed from the efficiency measurements of the individual components.

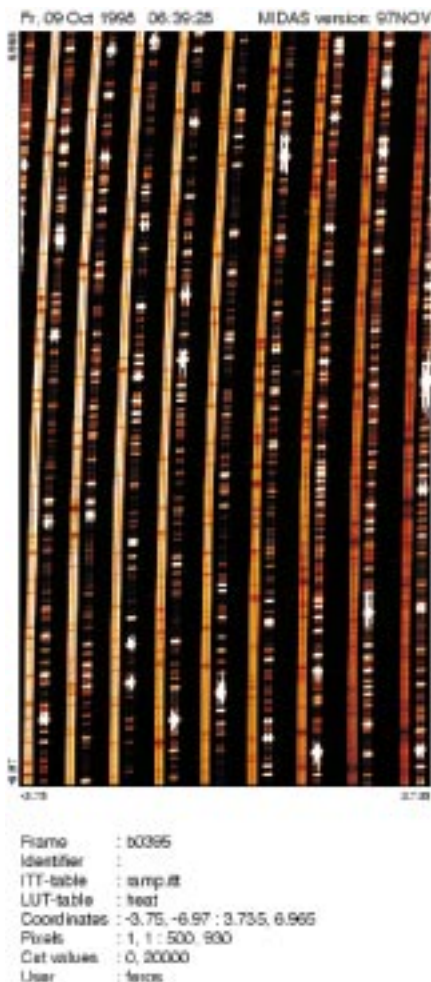


Figure 3: Central section of a raw spectrum of the radial-velocity standard  $\tau$  Ceti observed in the Object-Calibration mode of FEROS: each stellar spectral order is accompanied by the spectrum of the calibration lamp which is exposed simultaneously over the full exposure time of the object.

prove its high S/N capabilities during the commissioning observations. For this purpose, a series of spectra spread over the whole night, i.e., at different telescope positions, and with high photon counts have been obtained for the bright B8 Ia star  $\beta$  Ori. The S/N measured in the reduced single spectra is close to 700, which is consistent with the S/N expected from pure photon statistics. Averaging of 5 single  $\beta$  Ori exposures increased the S/N to about 1400.

### High-Precision Radial Velocities

To obtain a high long-term accuracy in radial-velocity measurements, FEROS has been equipped with the possibility to record simultaneously with the stellar spectrum the spectrum of the Thorium-Argon-Neon calibration lamp on the second fiber. This allows to monitor the residual motions of the spectrograph during the night and during the exposure. To explore the capabilities of this so-called Object-Calibration (OC) mode, the bright solar-type radial-velocity standard star  $\tau$  Ceti ( $\Delta v_{\text{rad}} < 3$  m/s) and the famous 51 Peg ( $\Delta v_{\text{rad}} = 57$  m/s,  $P = 4.2$  days) were

observed regularly during the two commissioning periods. Figure 3 shows a section of the first raw echelle spectrum of  $\tau$  Ceti obtained in the OC mode with FEROS.

Figure 4 shows the radial-velocity curve of  $\tau$  Ceti with 130 measurements over a period of 55 days. The radial velocities are obtained by simple order-by-order crosscorrelation of the 39 echelle orders of the object and of the simultaneous calibration fiber with respect to a corresponding reference spectrum. Neither special masks or templates for the star or for the calibration lamp have been used, nor the full wavelength calibration solution. With this simple approach, a radial-velocity dispersion of 21 m/s rms is achieved for this supposedly constant star. For 51 Peg, 30 measurements have been obtained and the residuals to the well-determined orbital curve show a rms of 29 m/s.

It is worth noting that the instrument was not working under the best and most stable conditions during the commissioning periods since numerous disturbing tests and optimisations had to be carried out during daytime. Therefore, we suppose that with the potential improvements from a dedicated software and from an improved stability of the environment, FEROS should be able to join the small club of instruments working in the  $< 10$  m/s domain. However, this is out of the scope of the FEROS contract and commissioning and, therefore, no further steps will be made in this direction by the FEROS consortium.

Alternatively, the second fiber is fed by the sky background nearby the object fiber (the fixed distance between the fibers is 50 arcsec). The Object-Sky (OS) mode in principle allows to subtract all sky contributions from the object spectrum, e.g. the night-sky emission lines in long exposures. The sky subtraction capabil-

ities of FEROS were tested by following an O star with few and broad lines with multiple 5-minute exposures at the end of the night into the twilight. The top two spectra of Figure 5 show the spectra recorded in the object and sky fiber shortly before sunrise with the stellar spectrum heavily contaminated by the bright sky background. After subtraction of the sky spectrum ('object - sky') the stellar spectrum is completely recovered. As comparison, the stellar spectrum obtained during the night ('object') is shown. Before subtracting the on-line reduced one-dimensional object and sky spectra, a constant factor of 0.95 had to be applied to the intensity scale of the sky spectrum. This factor reflects the slightly different flatfield illumination of the two fibers.

This result together with the reported FEROS flatfield capabilities is of high relevance, since the use of fibers in high-resolution spectroscopy has often been questioned on the basis of these problems. It is as well worth noticing that the FEROS system is very similar to the UVES fiber link as it will be mounted on the UT2 of the VLT. Therefore, we are confident that in this respect the FEROS commissioning results can be scaled to the VLT and UVES.

### CCD System

The thinned and back-illuminated  $2k \times 4k$   $15\mu\text{m}$  pixel EEV CCD with its excellent quantum efficiency (measured peak QE = 98% at 450 nm) contributes considerably to the high detection efficiency of FEROS. In combination with the Copenhagen CCD controller, a read-out noise of 3.7 and 3.5  $e^-/\text{pixel}$  for channel A and B is reached, respectively. Together with its high full-well capacity of 130,000  $e^-/\text{pixel}$  and the very low blooming as observed at strongly saturated

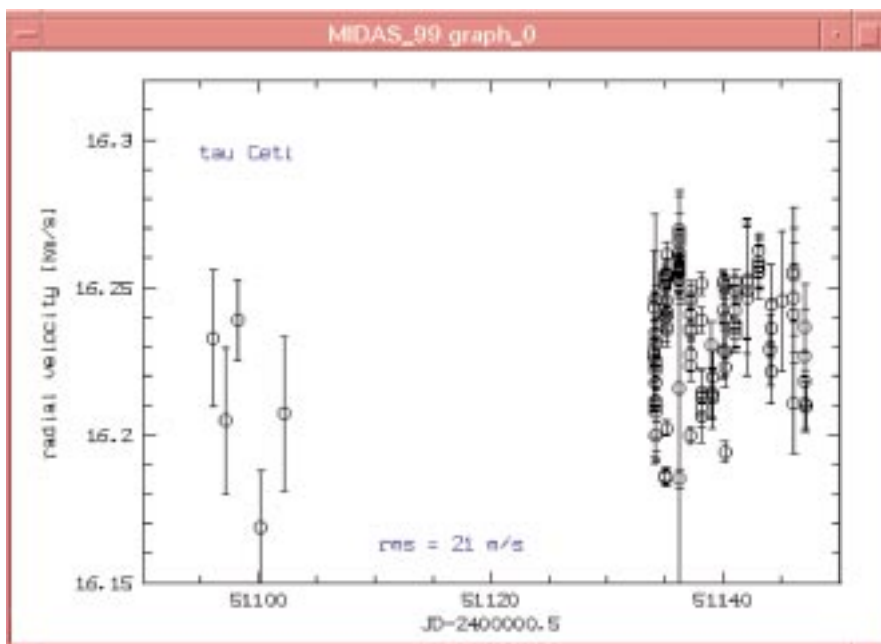


Figure 4: Radial velocity curve of the constant solar-type star  $\tau$  Ceti.

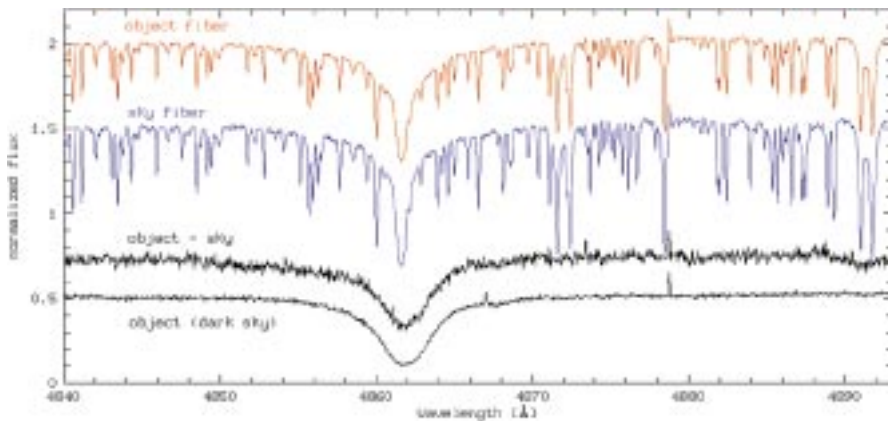


Figure 5: Skylight subtraction capability as tested on the bright O9 II star HR 3219 during the morning twilight.

spectral lines, the FEROS CCD seems to match perfectly the requirements of the instrument for both, low and high S/N observations.

Unfortunately, the CCD currently shows very bad cosmetics with several strong and numerous weak bad columns, the latter with the tendency to cluster into several neighbouring bad columns. Due to the high filling factor of the 2-dimensional echelle spectrum on the detector and the given orientation of the main dispersion direction along the 4k CCD columns, a considerable fraction of the 39 spectral orders is affected by the bad columns. The problem behind was traced down by the Optical Detector Team in Garching, which found that the cooling of the CCD chip is insufficient, i.e., the specified operating temperature of  $-120^{\circ}\text{C}$  is not reached by the continuous-flow dewar of FEROS. This would explain why the numerous bad columns do not freeze out leaving the CCD with the two bad columns as reported by the manufacturer. An explanation by insufficient cooling goes in line with the observed high dark current of the FEROS CCD. Long dark exposures show strong structures with peak values for the dark current of 10 to 20  $e^-/\text{hour}/\text{pixel}$ . The structures in the dark frames are found to be stable over several weeks, which allows to correct long science exposures for this structured background. Obviously, the high dark current is at the moment the limiting factor for FEROS for long low-S/N exposures since the noise contribution from the dark current becomes considerably higher than the very low read-out noise of the system.

To improve the performance of the CCD system, an upgrade of the dewar is planned for February 1999. The aim is to increase the heat conduction from the chip to the cold-head and to minimise the heat conduction through the electrical cabling. We hope that when you read these lines, FEROS is already back to operation and now presents its full performance with the upgraded CCD system.

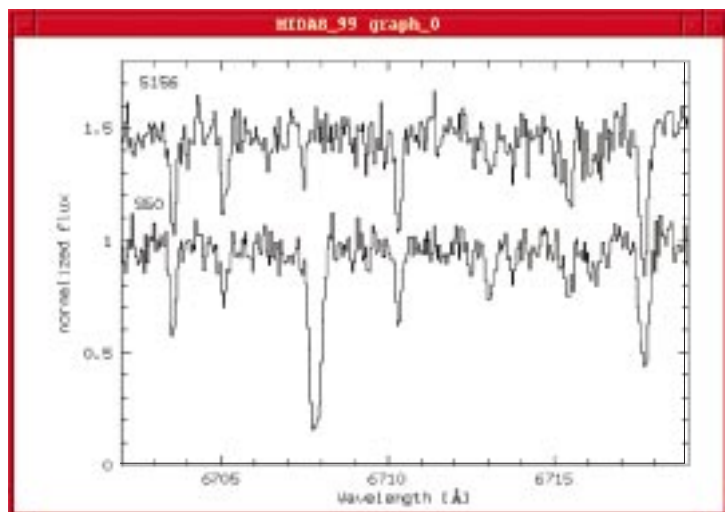
To complete this section it is worth mentioning that the FEROS spectra taken with the thinned  $2k \times 4k$  EEV CCD show the unavoidable strong fringes in the red starting at about 700 nm. The ampli-

tudes of the fringe patterns are strong with measured maximum values of more than  $\pm 20\%$ . Thanks to the fiber feed and the long-term stability of the FEROS spectrograph, the fringes are corrected to a level of clearly better than 1% just by flatfielding. This is also true for science exposures taken at different positions on the sky and using the flatfields taken in the afternoon during the initialisation of the on-line data reduction software.

### Data-Reduction Software and Pipeline

FEROS was delivered with a dedicated data-reduction software (DRS) developed at Heidelberg. This DRS is implemented in the ESO-MIDAS system as a new context named *feros* and will be distributed with the MIDAS package from version 98NOV on. The DRS is designed as a very general echelle-reduction software but is optimised for FEROS in the sense that it takes into account the double fiber feed of the spectrograph, the use of the two fibers with a double image slicer, and the strong curvature of the or-

Figure 6: Spectra of two K giant stars in the metal poor cluster Berkeley 21. Both stars have a V magnitude of 15.6 and a V-I around 2 mag. The exposure times are  $2 \times 1$  hour for each object; the S/N is estimated to  $> 20$  in this spectral region.



**PLEASE NOTE:** An on-line searchable database with all FEROS spectra obtained during the commissioning period and the first guaranteed time (dataset not complete yet) is now available on the WWW:

<http://www.lsw.uni-heidelberg.de/~akauffer/Feros/ferosDB/search.html>  
Note that the data obtained during the commissioning period are Public.

ders caused by the prism crossdisperser.

In addition to the standard routines for echelle data reduction, the FEROS DRS includes the possibility for standard and optimum extraction of the orders with and without cosmic rays spots clipping. For this, the advantage of the stable fiber feed can be used to define the necessary cross-order profiles just on the high S/N flatfield instead of the science frames. The tests during the commissioning showed that the gain in S/N with the optimum extraction corresponds to the theoretically expected – even for the complex wavelength dependent image-slicer cross-order profiles.

Further, the wavelength calibration is working with a global approach, i.e., a single multi-parameter function including the order number as one parameter is fitted to the positions of all automatically identified emission lines of the Thorium-Argon-Neon calibration lamp. This approach leads to a very stable over-all wavelength solution. The residuals between the known wavelengths of the identified lines and the fitted wavelengths show a stable rms value of  $< 3 \text{ mÅ}$ . The residuals display no trends with position and wavelength, which is a good indication that the used global fit formula (which is directly based on the grating equation) includes all relevant terms.

An important feature for the data reduction of highly stable fiber-linked echelle spectrographs is the well-defined blaze function for each echelle order. Since the light paths through the spectrograph for object and calibration exposures are to a high level exactly the same, the blaze correction can be done by flatfielding only. The quality of the blaze correction is best checked by the match of the flux levels of the overlapping regions of the contiguous echelle orders. In case of FEROS it is found that the match is on a level of better than 1%. This is a prerequisite to

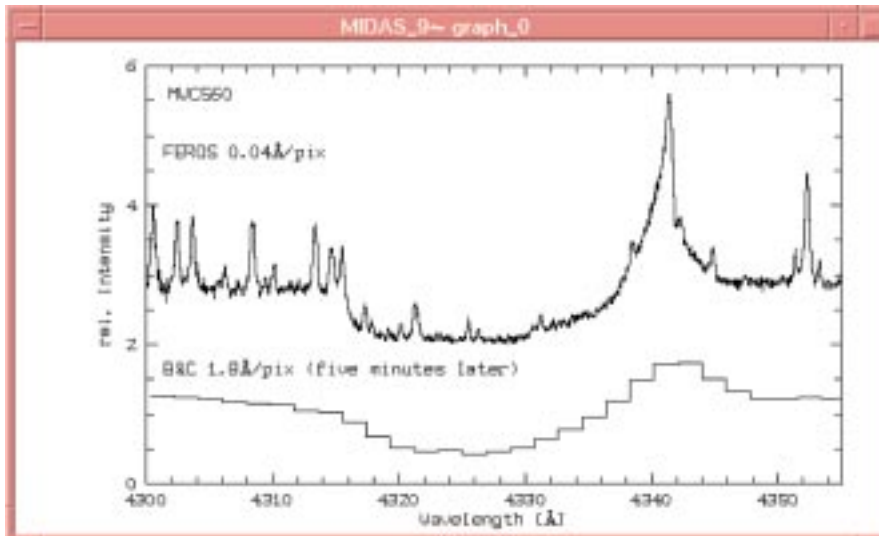


Figure 7: Spectra of the symbiotic star MWC 560 as obtained with FEROS (top,  $t_{exp} = 15$  min) and shortly after with the B&C (bottom,  $t_{exp} = 30$  sec). In between, only the slit unit was moved between the corresponding two positions.

apply routinely the merging of the wavelength calibrated echelle orders into a single and complete one-dimensional spectrum as done by the FEROS on-line DRS.

The FEROS on-line DRS pipeline as installed at the ESO 1.52-m telescope is an extension to the `feros` context. The on-line DRS is initialised with a set of calibration exposures taken daily before sunset. The initialisation programme provides the DRS with all frames (e.g. extracted flatfields) and tables (e.g. order positions, dispersion coefficients) for the coming night. During the observations, each incoming spectrum is archived on tape and processed according to its descriptor information, e.g., science frames are completely reduced into a flatfielded, wavelength-calibrated, barycentric-corrected, and merged one-dimensional spectrum, which allows the observer to inspect the spectrum about 6 minutes after the shutter is closed (using one-channel CCD readout and optimum extraction). Figure 6 shows the spectra of two faint metal poor stars which have been reduced by the on-line DRS with optimum extraction.

### Observing with FEROS

The new FEROS instrument has been integrated in the existing telescope and B&C instrument environment in the ESO 1.52 control room. The user will find one additional Linux PC controlling the new

common calibration unit for B&C and FEROS and the FEROS CCD, which uses the Danish BIAS software as known from the earlier days of DFOSC at the Danish 1.54-m telescope. The B&C exposures are still defined on the nearby HP 1000 system. Both, FEROS and B&C transfer their CCD frames to the HP instrument workstation where the FEROS on-line DRS and the B&C quick-look software are running in parallel on two different workspaces.

The change between the two instruments is very simple and requires only a manual movement of the new slit unit between the two corresponding positions. Figure 7 gives a nice demonstration of the possibility to use both instruments shortly one after the other. The figure shows the H $\beta$  line of the symbiotic star MWC 560 as obtained in high spectral resolution with FEROS and in low resolution with the B&C a few minutes later after a change of the slit unit. The change between the two instruments is currently not offered to the observers but it is easy to imagine scientific programmes which could gain from this symbiosis of these two in a certain sense complementary instruments. For example, for the first time high-quality high-resolution spectrophotometric programmes could be carried out easily by combining flux-calibrated low-resolution B&C spectra with the spectral details as obtained from FEROS.

The experience from several test observing nights with FEROS at the ESO 1.52-m telescope showed that some effort is needed to reach always the maximum possible performance of FEROS in combination with the ESO 1.52-m. Particularly, it turned out that a proper focusing of the telescope on the fiber apertures is crucial to feed a maximum of light to the fibers. This is due to the use of microlenses in the focal plane which convert the slow  $f/15$  telescope beam into a quite fast  $f/4.5$  beam that is naturally more sensitive to defocus. Also bad seeing of more than 1.5 arcsec considerably affects the efficiency of the telescope + instrument system. Together with a bad telescope focus quickly half of the photons from the object are lost for the spectrograph.

Apart from the focus, the expected S/N for different environmental conditions is quite reliably estimated with the FEROS exposure-time calculator (ETC).

### Further Information

All information concerning the status of the instrument (e.g. the CCD upgrade) and the preparation and execution of observations with FEROS (e.g. the ETC and the User Manual) can be found on the corresponding 2p2-team homepage<sup>1</sup>. In addition, this page provides links to more pictures and reports on the installation and commissioning phases of the FEROS instrument.

### Acknowledgements

Commissioning being at the end of the 'food chain', we would like to thank here all the people actively involved in the FEROS installation and commissioning at La Silla: Our special thanks go to the 2p2-team, Wolfgang Eckert and his mechanics team, the detector group, the optics lab with Alain Gilliotte and Roberto Tighe, and Fernando Luco and the infrastructure support team.

Further big thanks go to the FEROS PI, Bernhard Wolf, and the FEROS teams in Heidelberg and Copenhagen, and the detector group in Garching. It is thanks to all their efforts that it was possible to build FEROS and to get it operational so quickly.

<sup>1</sup><http://www.la.eso.org/lasilla/Telescopes/2p2T/EIp5M/FEROS/index.html>

A.Kaufer@lsw.uni-heidelberg.de

## Monitoring of the Atmospheric Sodium above La Silla

N. AGEORGES, National University of Ireland, Galway; Physics Department, Galway, Ireland

N. HUBIN, ESO

### 1. Introduction

This work corresponds to preparatory work for the laser guide star adaptive optics system planned for the VLT at

Paranal. In this framework ESO and the National University of Ireland, Galway, are collaborating within the Training and Mobility of Researcher programme on "Laser guide star for 8m class tele-

scopes", funded by the European Commission.

In Laser Guide Star (LGS) Adaptive Optics (AO), a laser is used to excite the mesospheric (90 km altitude) sodium